Accepted Manuscript

Unusual, basin-scale, fluid-rock interaction in the Palaeoproterozoic Onega basin from Fennoscandia: preservation in calcite δ ^{18}O of an ancient high geothermal gradient

A.E. Fallick, V.A. Melezhik, A.T. Brasier, A.R. Prave

PII: S0301-9268(16)30091-2
DOI: http://dx.doi.org/10.1016/j.precamres.2016.06.001
Reference: PRECAM 4522

To appear in: *Precambrian Research*

Received Date: 26 April 2016
Accepted Date: 1 June 2016

Please cite this article as: A.E. Fallick, V.A. Melezhik, A.T. Brasier, A.R. Prave, Unusual, basin-scale, fluid-rock interaction in the Palaeoproterozoic Onega basin from Fennoscandia: preservation in calcite δ ^{18}O of an ancient high geothermal gradient, *Precambrian Research* (2016), doi: http://dx.doi.org/10.1016/j.precamres.2016.06.001

This is a PDF file of an unedited manuscript that has been accepted for publication. As a service to our customers we are providing this early version of the manuscript. The manuscript will undergo copyediting, typesetting, and review of the resulting proof before it is published in its final form. Please note that during the production process errors may be discovered which could affect the content, and all legal disclaimers that apply to the journal pertain.

ACCEPTED MANUSCRIPT

Unusual, basin-scale, fluid-rock interaction in the Palaeoproterozoic Onega basin from Fennoscandia: preservation in calcite $\delta^{18}O$ of an ancient high geothermal gradient

A.E. Fallick[1], V.A. Melezhik[2], A.T. Brasier[1,3*], and A.R. Prave [4]

1. Isotope Geosciences Unit, SUERC, Rankine Avenue, East Kilbride G75 0QF, Scotland, U.K.
2. Norwegian Geological Survey, Leif Eirikssons vei 39, N-4791, Trondheim, Norway.
3. School of Geosciences, Meston Building, University of Aberdeen, Old Aberdeen, AB24 3UE, Scotland, U.K.
4. Department of Earth and Environmental Sciences, St. Andrews University, St. Andrews, Fife KY16 9AL, Scotland, U.K.

*corresponding author. Email: a.brasier@abdn.ac.uk; tel: 01224 273449

Abstract

A variety of carbonates of different geneses, as indicated by petrography and geochemistry, are found throughout 400m of the volcano-sedimentary rocks of the Zaonega Formation of Palaeoproterozoic age in the Onega Basin of Fennoscandia. Following intensive sampling and analysis of varied calcites from drillcore recovered during the ICDP FAR-DEEP program, we report a highly unusual depth distribution of calcite oxygen isotope values ($\delta^{18}O_{cal}$). Unprecedentedly for such rocks, the $\delta^{18}O_{cal}$ values over the full depth interval of 400m are strongly linearly correlated with depth (r^2 = 0.9015, n=178). We propose that this is the result of major oxygen isotope resetting through water-

ACCEPTED MANUSCRIPT

rock interaction with a fluid of relatively constant oxygen isotopic composition ($\delta^{18}O_w$). In this model, the observed linear $\delta^{18}O_{cal}$-depth relationship is then a consequence of the increase in temperature with depth because of the background geothermal gradient. Minor deviations from the overall linear trend are likely due to bed-scale geological factors including locally high impermeability, and oxygen isotope modification of $\delta^{18}O_w$ by comparatively intense water-rock interaction.

Were the observed $\delta^{18}O_{cal}$ values to have been reset during the greenschist facies Svecofennian metamorphism which affected the rocks at c. 1800Ma, the implied geothermal gradient of ~ 560°C km^{-1} is geologically unreasonable and, accordingly, this hypothesis is ruled out. Rather, the $\delta^{18}O_{cal}$ variation of 5‰ over 400m implies a near-surface depth for the rocks during fluid interaction, and this is consistent with a surface-derived origin of the infiltrating fluid ($\delta^{18}O_w$ ~ -13.6‰ for a surface temperature of 15°C and geothermal gradient of ~ 52 °C km^{-1}). It is speculated that the fluid accessed the carbonates from the basin edge by bed-parallel rather than cross-formational flow.

There is an intriguing distribution of Na in the sedimentary rocks of the Zaonega Formation. Sodium is relatively abundant in rocks below a certain depth (the Lowermost Dolostone at ~258m), but rare in shallower sequences. It is argued that this distribution did not originate with the basin-scale fluid-rock interaction documented above, but may rather be the result of evaporite dissolution, and subsequent redistribution of soluble elements during fluid flow associated with the syndepositional emplacement of basin-wide igneous rocks.

Introduction

Oxygen isotope ratios of carbonate rocks can record parent fluid temperatures at the time of mineral precipitation (Urey, 1947). This includes, for example, shallow marine carbonates precipitated from seawater (see, e.g. Veizer, 1992). However, in older rocks it is often apparent that the carbonate oxygen isotope values have been re-set (Veizer, 1992). This happens whenever oxygen atoms exchange between the rock and basinal fluids, but particularly when carbonate

ACCEPTED MANUSCRIPT

minerals dissolve and re-precipitate during burial. Given sufficiently intense water-rock interaction, fluid $\delta^{18}O$ ($\delta^{18}O_w$) will change during prolonged post-depositional reactions, governed by mass and isotopic balance and the thermal regime; a key concept is the *effective* fluid-rock ratio (see, e.g. the discussion in Clauer et al., 2014). A complex distribution of final mineral $\delta^{18}O$ values is therefore not unusual. Despite numerous studies of burial diagenesis of carbonate rocks, we are not aware of any reported case of carbonate oxygen isotopes consistent with a uniform increase in temperature with depth (i.e. preservation of an ancient geothermal gradient).

The Palaeoproterozoic Onega Basin of Fennoscandia hosts the Zaonega Formation (ZF), a c. 900m-thick succession of immature siliciclastic rocks, carbonates, cherts and mafic tuffs and basalts, which are all intruded by gabbroic sills (Melezhik et al., 2012; Črne et al., 2013a,b; 2014). The International Continental Drilling Project (ICDP) FAR-DEEP Holes 12A and 12B were drilled in the same location (Latitude 62.4947N, Longitude 35.2887E) to provide a single continuous section through the volcano-sedimentary succession of the ZF (Fig. 1). These two cores are here referred to as Hole 12AB. ICDP FAR-DEEP Hole 13A (Latitude 62.5891N, Longitude 34.9273E) was drilled 25km to the north-west of 12AB and represents a separate section that partially overlaps with Hole 12AB (Melezhik et al., 2012; Fig. 1). The base of the uppermost dolostone unit in Cores 13A (76.6 m) and 12AB (9.3 m, 'Dolostone-Chert Member'; Fig. 2) was used as the lithostratigraphic marker boundary for correlation between 12AB and 13A (Črne et al., 2013a,b; 2014). In addition, a lithological interval with several thin beds, containing specific black and pale brown "clay balls" up to 2cm in size, was suggested as another marker interval for the correlation of Cores 13A (183–159 m) and 12AB (180–160 m).

Carbonates are found throughout 0.4 km of section in 12AB and 13A, and are described in detail by Črne et al. (2014) and Melezhik et al. (2015). Geochemical properties of carbonate are here generically identified by the subscript 'carb', and when samples are mineralogically assigned to calcite (through having carbonate Mg/Ca <0.1) by the subscript 'cal' (see Fig.2 and text below). Our focus here is on the post-depositional diagenetic history of the ZF, meaning on the calcites rather than the dolomites (Črne et al., 2014). The

ACCEPTED MANUSCRIPT

lowermost dolostone (hereafter LMD) in Core 12AB is a carbonate-shale bed at 258–233 m. Below this depth there are few dolostones, but thin, layered or massive calcitic beds. On a micro- to macro-scale the calcite is here intergrown in xenomorphic masses containing chamosite, albite, K-feldspar, quartz, mica and minor tremolite (Melezhik et al., 2015). Črne et al. (2014) described these as patches of irregular-shaped calcite with numerous embayments, tightly intergrown with albite. The LMD interval itself includes variably calcitised dolostones exhibiting granular, massive and/or bedded/layered textures. Calcite-filled extension cracks are common in this section. Carbonate rocks occurring above the LMD range from pure dolomitic, through mixed dolomitic-calcitic, to calcitic in composition. Some of the dolomite textures are remininscent of microbially-generated structures (Melezhik et al., 2015), whereas calcite is commonly found on the dolostone bed margins, where it is likely the result of dedolomitisation (Črne et al., 2014). Calcite in the bed centres is a more minor constituent of rocks above the LMD. Here scanning electron microscopy reveals such calcite to be a relatively late-stage overgrowth on earlier-formed dolomite crystals (Črne et al., 2014).

Detailed petrography throughout the ZF stratigraphy (Črne et al., 2014; Melezhik et al., 2015) indicates several generations of calcite. Črne et al., (2014) viewed these as dominantly the result of hydrothermal processes shortly after deposition of the Zaonega Formation sediments, and likely linked to emplacement of a basin-wide gabbro body. Melezhik et al. (2015) interpreted three pre- to syn-metamorphic generations of calcite, and one later stage of diagenetic calcite formation. According to the latter authors, the earliest generation was linked to petroleum migration and was petrified in pyrobitumen-calcite veins (Fig. 5A). Pre-metamorphic calcitisation was caused by hydrothermal fluid circulation associated with the syndepositional emplacement of the basin-scale gabbro sill (Melezhik et al., 2015). Syn-metamorphic calcitisation caused by dolomite-silicate reaction was widespread (Fig. 5B,C) in Cores 12AB and 13A. The final generation includes calcite occurring as porphyroblasts that in the view of Melezhik et al. (2015) are superimposed on metamorphic fabrics. In shales, this final calcite phase appears as replacive,

ACCEPTED MANUSCRIPT

pancake-like crystals (Fig. 5D). In sandstones, Melezhik et al. (2015) report that it forms irregular porphyroblasts superimposed on granoblastic and meta-psammitic texture (Fig. 5E). In interbedded gritstone-sandstone-siltstone, porphyroblastic calcite develops preferentially in coarser lithologies. Calcite has been observed as large porphyroblasts completely replacing feldspar and quartz in gritstone-sandstone, whereas fine-grained, organic-rich siltstone remains largely unaffected (Fig. 5F–H). Melezhik et al. (2015) note this late calcite apparently cuts across bedded, metamorphosed sediments and shows no apparent foliation, which would require that it post-dates the c. 1.8 Ga Svecofennian orogeny .

Geochemical criteria have proven useful for subdividing the calcites when encountered in whole-rock powders (Melezhik et al., 2015). This is because many low Mg calcites in these ZF cores are associated with low whole rock Mg/Ca ratios ($Mg/Ca_{wr)}$ of <0.1), and these generations were those plausibly originally precipitated as calcite. In contrast, other weak acid-soluble, low Mg/Ca ratio samples (i.e. calcite, with carbonate Mg/Ca_{carb}<0.1) come from powders with higher whole-rock Mg/Ca ratios as measured by XRF (i.e. Mg/Ca_{wr} >0.1). The weak acid-soluble calcite in these rock powders is thought to have formed through the metasomatic alteration of dolostone.

In this study we pay particular attention to the low Mg carbonates (with carbonate Mg/Ca<0.1) that were deposited as calcite, together with those formed through dolostone alteration (where Mg/Ca_{wr}>0.1 but Mg/Ca_{carb}<0.1), i.e. all samples that are now calcite. We report an extraordinary linear relationship between all 178 such calcite $\delta^{18}O$ and depth values in Core 12AB (see data in Table 1, Figure 2, and later), that must have developed post-lithification. We hypothesise that this linearity reflects establishment of calcite $^{18}O/^{16}O$, and resetting (perhaps during dedolomitisation) of the older dolomite $\delta^{18}O$ values, in an ancient geothermal gradient that was relatively high.

ACCEPTED MANUSCRIPT

The lithostratigraphy and depositional age

In summary, following Črne et al. (2013a,b; 2014), the ZF as sampled in Hole 12AB consists from the bottom upwards of the *Greywacke Member* (498-250m) which includes the significant basin-wide gabbroic Magmatic Unit B (484-414m), the *Dolostone-Greywacke Member* (250-179.7m), the *Mudstone-Limestone Member* (179.7-9.3m) and the topmost *Dolostone-Chert Member*. Melezhik et al. (2015) suggested a parallel subdivision by recognising an additional unit termed the *Lowermost Dolostone* (LMD, 258–233 m, Fig. 2).

A maximum age for the ZF has been imprecisely constrained at 2090 ± 70 Ma by a Pb-Pb technique on dolomite of the underlying Tulomozero Formation (Ovchinnikova et al., 2007). Hannah et al. (2008) reported a preliminary Re–Os age of ca. 2050 Ma obtained on organic matter from the upper part of the ZF. A minimum age for the ZF of ca. 1980 Ma has been constrained by several whole-rock and mineral Sm–Nd and Pb–Pb isochrons on the Konchozero mafic-ultramafic sill which was emplaced in the upper part of the ZF but considered to be co-magmatic with the overlying Suisari Formation (Puchtel et al., 1992; Puchtel et al., 1998). The rocks were metamorphosed in the greenschist facies during the c. 1800 Ma Svecofennian orogeny (Volodichev, 1987).

Analytical methods

Detailed petrographic characterisation was carried out at NGU, including use of SEM-BSE and CL imaging techniques (Črne et al., 2014). Samples cut from ICDP FAR-DEEP cores 12A and 12B were then crushed to produce whole-rock powders. Aliquots of these homogenous powders were used for elemental and carbonate stable isotope analyses.

Major and trace elements of whole-rock powders were first analyzed at the Geological Survey of Norway NGU by X-ray fluorescence spectrometry using a PANalytical Axios at 4 kW. Elemental concentrations for the carbonate component were also determined on acidified extracts (cold 10% HCl) of sub-aliquots of the powders by inductively coupled plasma-atomic emission

ACCEPTED MANUSCRIPT

spectrometry (ICP-AES) using a Thermo Jarell Ash ICP 61. Potential issues of leaching of Mg or Ca from silicate phases by the 10% HCl are not thought to be significant (and were monitored by Si and Al concentrations in the leachate), and no correlation is seen between whole rock and carbonate Mg/Ca.

Stable carbon and oxygen isotopes analyses were performed at the Scottish Universities Environmental Research Centre (SUERC). Approximately 1 mg aliquots of the powders were placed in individual tubes and reacted overnight with phosphoric acid at 70˚C. Isotopic ratios in the evolved CO_2 were measured on either Micromass PRISM II or AP2003 mass spectrometers. Repeat analyses of NBS-19 and internal calcite standards are generally better than ±0.2‰ for carbon and ±0.3‰ for oxygen. Carbon and oxygen isotopic values of calcites are reported as $\delta^{13}C_{cal}$ and $\delta^{18}O_{cal}$ and discussed in the conventional delta notation relative to V-PDB and V-SMOW, respectively.

Major, trace element and C- and O-isotopic data are presented in Table 1 (Core 12AB) and Table 2 (Core 13A).

Presentation of $\delta^{18}O_{cal}$ data

The variation of measured calcite $^{18}O/^{16}O$ ($\delta^{18}O_{cal}$) for all 178 samples throughout 0.4 km of section in Core 12AB is shown in Fig. 2B tied to the lithology of Črne et al. (2013a) modified via recognition of the LMD. It is immediately apparent that in Core 12AB (and this is also true to a lesser extent in Core 13A) there exists a very strong trend of $\delta^{18}O_{cal}$ decreasing with depth (illustrated in Fig. 3), which is coherent over the entire 0.4 km of studied section and is independent of the interpolation of non-carbonate-bearing clastic and igneous rocks between carbonate-bearing lithologies. The r^2 value of 0.90 implies that 90% of the variation in $\delta^{18}O_{cal}$ can be explained by the depth dependency. This is rather remarkable and we know in the literature of no similar occurrence for rocks like these over this scale. There is no compelling evidence of displacement of $\delta^{18}O_{cal}$ from the overall trend at the boundaries of the calcites with igneous rocks, in contrast to the variation of measured organic matter $^{13}C/^{12}C$ (see e.g. Fig. 2 of Qu et al., 2012). For calcites, there is no correlation

ACCEPTED MANUSCRIPT

between $\delta^{13}C_{cal}$ and $\delta^{18}O_{cal}$, nor between $\delta^{13}C_{cal}$ and sample depth (Fig. 2C) throughout 0.4 km of section.

Interpretation

Because we wish to examine the relationship between $\delta^{18}O_{cal}$ and depth (z), it is imperative that there is no ambiguity about the sample depth. Although Core 13A also shows a significant trend of calcite $\delta^{18}O_{cal}$ decreasing with depth, below for two reasons we consider only Core 12AB data. Firstly, there is no precise and unambiguous chronostratigraphic correlation currently available for these two cores, albeit plausible attempts have been made as discussed above; this implies that adopting common z scale involves additional assumptions, which we are reluctant to do. Secondly, Core 12AB is represented by a larger data base covering a significantly greater depth interval than Core 13A.

For the Core 12AB data shown in Fig. 3 there are regions in which some scatter occurs around the overall trend (estimated to be about ±1‰), particularly around 150m depth, and these probably reflect local heterogeneities (e.g. permeability contrasts) influencing the overall circumstances of water-rock interaction. For the modelling exercise we are about to undertake it would be possible to filter out some of the geological 'noise' by excluding these values, and considering separate depth intervals, so defining a more accurate relationship between $\delta^{18}O_{cal}$ and depth, but we are at the moment more interested in the overall efficacy of our approach, and so proceed with the entire database illustrated in Fig. 3. Later refinements are conceivable if the general approach is shown to have merit.

For the depth (z) in kilometres the best-fit line through the data illustrated in Fig. 3 is:

$$\delta^{18}O_{cal} = 17.3 - 13z, \text{ with } r^2 = 0.9015, n=178 \quad [1]$$

which is statistically significant well above the 99.9% level. By differentiation with respect to depth (z) we obtain:

ACCEPTED MANUSCRIPT

$$\partial\,\delta^{18}O_{cal} / \partial\, z = -13 \text{ (‰ km}^{-1}\text{)}. \qquad [2]$$

Let us assume that the calcite $\delta^{18}O_{cal}$ of the entire suite was set by isotopic equilibrium with a fluid of constant oxygen isotopic composition ($\delta^{18}O_w$). The oxygen isotope fractionation factor between calcite and water is described by (Friedman and O'Neil, 1977):

$$\delta^{18}O_{cal} - \delta^{18}O_w = a\,T^{-2} + b \qquad [3]$$

where T is temperature °K, and **a**, **b** are numerical constants, with **a** = $2.78*10^6$, and **b** = -2.89.

Differentiating equation [3] with respect to depth (z):

$$\partial\,\delta^{18}O_{cal}/\partial\, z - \partial\,\delta^{18}O_w/\partial\, z = -2aT^{-3}\ \partial\, T/\partial\, z$$

and the assumption of constant $\delta^{18}O_w$ ensures that $\partial\,\delta^{18}O_w/\partial\, z = 0$ (see later for a relaxation of this restriction). Also, since T (°K)=t (°C) + 273, then we have that $\partial\, T/\partial\, z = \partial\, t/\partial\, z$, which is the geothermal gradient. Therefore, substituting and rearranging:

$$\partial\, t/\partial\, z = (-T^3/2a)\ \ \partial\,\delta^{18}O_{cal}/\partial\, z \qquad [4]$$

Since we have evaluated $\partial\delta^{18}O_{cal}/\partial z$ as -13‰ km^{-1} in [2], the relationship in equation [4] allows us to investigate the (T, $\partial t/\partial z$) conditions under which the linear correlation between $\delta^{18}O_{carb}$ and depth illustrated in Figs. 2B and 3 might have been established. For example, under the greenschist facies of the 1800 Ma Svecofennian metamorphism, let us assume t ~ 350°C, then T ~ 623°K and the observed variation of $\delta^{18}O_{cal}$ with depth of -13‰ km^{-1} would require a geothermal gradient of ~560 °C km^{-1}. That is, because oxygen isotope fractionation is low at high temperature (scaling as T^{-2}), in order to reproduce the observed change in $\delta^{18}O_{cal}$ of 5‰ over 0.4 km requires a geologically

ACCEPTED MANUSCRIPT

unreasonable geothermal gradient (see also later discussion). In addition, calculation of $\delta^{18}O_w$ from equation [3] for a temperature of 350°C and $\delta^{18}O_{cal}$ of 17‰ yields an unlikely value (>12.5‰). We infer that the fluid-rock interaction process resetting $\delta^{18}O_{cal}$ did not accompany the metamorphism and conclude that it was a lower temperature process which established the observed depth variation of $\delta^{18}O_{cal}$.

Other geologically reasonable pairs of values of temperature and geothermal gradient, which satisfy equation [4] for **a**=2.78*10^6 and the observed calcite oxygen isotopic gradient with depth (Figs. 2B and 3) of -13‰ km^{-1}, have been calculated and for heuristic reasons are plotted in Fig. 4; they can be investigated by substitution into equation [4] and are approximated by $\partial t/\partial z = 40 + 0.8t$. For example, at a temperature of ~40°C (and geothermal gradient of ~70°C km^{-1}) we can then calculate $\delta^{18}O_w$ from equation [3] as ~-8.5‰. Alternatively, at a lower temperature of ~15°C (and more modest geothermal gradient of ~52°C km^{-1}) we can calculate $\delta^{18}O_w$ from equation [3] as ~-13.6‰.

Recall that we have scatter in Fig. 3 of ±1‰ and this would translate directly into scatter in calculated $\delta^{18}O_w$. We do not argue for the accuracy and appropriateness of these individual values of the respective parameters at the time of fluid-rock interaction; rather, we merely suggest that a model of this type can reasonably reproduce the observed depth trend of $\delta^{18}O_{cal}$ with geologically acceptable values of geothermal gradient and water isotopic composition.

The geothermal gradient, the source of the fluid responsible for establishing $\delta^{18}O_{cal}$, and fluid flow models.

We inferred in the previous section that the observed trend of $\delta^{18}O_{cal}$ with depth, interpreted as a consequence of the geothermal gradient and a constant $\delta^{18}O_w$, was not compatible with oxygen isotope resetting during Svecofennian greenschist facies metamorphism because the calculated geothermal gradient of 560 °C km^{-1} was geologically unrealistic. There are cases in the literature when

ACCEPTED MANUSCRIPT

very high temperature gradients have been calculated. For example, Cathles and Adams (2005), assuming a surface temperature of 15°C, calculated a temperature gradient of 360-400 °C km^{-1} for the Tri-State Mississippi Valley Type ore deposit district in SW Missouri. The situation here was that hot basin brines at 110-120 °C, likely transported long distances in deep aquifers, have been brought to near the surface in the continental interior by conduits that are structurally controlled. Ore was precipitated at ~0.25 km depth, leading to the apparently high calculated temperature gradient (Sangster et al., 1994). This model does not fit the volcano-sedimentary sequence of the Onega Basin rocks; there is no reported evidence for introduction of such mineralisation, and that which is observed, discussed in Melezhik et al. (2015), is of quite a different character and is dated to 1760±60 Ma, long after the Svecofennian metamorphism. This supports our previous conclusion that the calculated gradient of 560°C km^{-1} is geologically unreasonable for the Onega Basin situation.

It is possible to relax the assumption of constant $\delta^{18}O_w$ to produce the observed $\delta^{18}O_{cal}$ relationship if $\delta^{18}O_w$ varies linearly with depth. Assuming the implausible possibility of cancellation of non-linear variations in the depth relationships of $\delta^{18}O_w$ and temperature is excluded, then linear variation of $\delta^{18}O_w$ with depth means $\partial\, \delta^{18}O_w / \partial\, z$ is a constant and equation [4] is preserved with a numerical modification to -13‰ km^{-1} (additively, by the constant), and the argument proceeds as before. For a more complex and realistic variation of $\delta^{18}O_w$ throughout the mixed-lithology basin (for a basinal fluid modified by isotope exchange during water-rock interaction during burial, e.g. Egeberg and Aagard (1989)), it is theoretically possible to construct a complex thermal regime which still delivers a strictly linear variation of $\delta^{18}O_{cal}$ with depth, but this destroys the simple elegance of the model presented above and the fortuitous cancellation of temperature and $\delta^{18}O_w$ effects seems physically implausible. For any temperature less than 100°C, the calculated $\delta^{18}O_w$ is <0‰ and so the fluid is surface-derived, in the sense that it is seawater/meteoric water - not a geothermal or other crustal fluid, nor one of metamorphic or igneous origin

ACCEPTED MANUSCRIPT

(Sheppard, 1986; note that a Shield brine is permitted but geologically unlikely). This argument is robust in the context of debate about the oxygen isotopic composition of seawater in the geological past (see Jaffres et al. (2007), for example).

To account for a simple relationship between $\delta^{18}O_w$ with depth and minimise the impact of changing $\delta^{18}O_w$ through water-rock interaction during penetration of the near-surface derived fluid, one could speculate that infiltration parallel to bedding, perhaps from the basin edge, was more likely than cross-formational fluid flow. Whilst the latter is not unknown in sedimentary basins (e.g. Sullivan et al., 1990) it is distinguished by its novelty compared to ingress of meteoric water, along conduits parallel to bedding, from the basin flanks (e.g. Haszeldine et al., 1992). In a major review of fluid flow in the upper 20km of the continental crust Cathles and Adams (2005) emphasise that for the upper 3km, aqueous fluids are normally at close to hydrostatic pressure and fluid flow is, in the absence of structural features such as doming or faults and cracks, preferentially along lateral high permeability channels. Fluid drive could then be because of hydrostatic head, rather than being hydrothermally-forced. The strong links between burial diagenesis and metasomatism of basinal sediments (including cement precipitation, dolomitization, calcitization, and albitisation of feldspars), migration of hydrocarbons and potential hydrothermal ore deposition, with some startling similarities to the Onega Basin, have been emphasised by Hardie (1991 especially p.156 and 163) in his review of evaporites and their significance.

We conclude that a straightforward explanation of the observed linear decrease of $\delta^{18}O_{cal}$ with depth is that the fluid responsible for establishing $\delta^{18}O_{cal}$ was introduced from outwith the basin, had $\delta^{18}O_w$ <0‰ and was surface-derived.

Timing of fluid-rock interaction

There are two known times when the rocks described in Fig. 2 were sufficiently close to the Earth's surface to have a thermal regime capable of reproducing the observed $\delta^{18}O_{cal}$ trend with depth (and, of course, an

ACCEPTED MANUSCRIPT

unconstrained number of occasions in between). These are, firstly, close to the time of sedimentation of the topmost 'limestone' of the Mudstone-Limestone Member, and secondly, the present-day. The former can be excluded if one accepts that the observed depth-$\delta^{18}O_{cal}$ trend overprints any diagenetic, igneous-related and even metamorphic resetting. Linking petrography with geochemistry, we infer that the fluid responsible for the latest calcite generation (post-metamorphic according to Melezhik et al., 2105; Fig. 5F-H) also caused substantial re-setting of the earlier carbonate $\delta^{18}O$ signals. Consequently, in a model where the $\delta^{18}O_{cal}$ depth-trend is established by the geothermal gradient in a low temperature regime, then the fluid infiltration occurred sometime between c. 1800 Ma and the present day, but otherwise temporally unconstrained. Any link to the c.1760 Ma metasomatic mineralisation mentioned in Melezhik et al. (2015) would be speculation. The exhumation which brought the rocks close to the surface could also have facilitated the incursion of contemporaneous near-surface, likely meteoric, fluids (see e.g. Jenkin et al. 1994). This can be seen as likely the last major fluid-rock interaction event to significantly affect the calcite $\delta^{18}O$, and the exceptional measured $\delta^{18}O_{cal}$ depth profile has thus been preserved.

Fluid-Rock interaction related to Na mobility and albitisation

Filippov et al. (1994) noted that the lower part of the ZF (the 'sodic-series') was enriched in sodium, and Melezhik et al. (2013; 2015) speculated that albitisation of some rocks of the Greywacke Member occurred when hydrothermal systems driven by the heat associated with emplacement of the ~70m thick Unit B gabbro (at 484 to 414m depth in 12AB) mobilized Na; the source of the element was envisaged (Melezhik et al., 2013) to be "either seawater or from a partially dissolved, thick halite bed present at the base of the Tulomozero Formation underlying the ZF". The recognition above that there was very plausibly a subsequent basin-scale fluid influx raises the issue of whether Na, and presumably other components such as sulfate, was subsequently

ACCEPTED MANUSCRIPT

remobilized (or, at a more extreme level, that albitisation and establishment of $\delta^{18}O_{cal}$ were related). This question is given some importance by the observation of Melezhik et al. (2015) that for Core 12AB samples below 258m, carbonate $\delta^{18}O$ and K_2O/Na_2O_{wr} co-vary (r = -0.3, n=82, >99%): this warrants further discussion of the Na distribution here.

The observed distribution of Na_2O^* is interesting, though not fully understood, least of all in relation to the lithostratigraphy. The whole database (all carbonates in Cores 12AB and 13A with the full range of Mg/Ca) shows a dramatic increase of Na_2O^* down depth below the lowermost dolostone (Fig. 2D). In Core 12AB calcites, Na_2O^* is below the detection limit of 0.1 wt.% for most of the analysed samples above 259.3 m (only 13 samples out of 104 had detectable values with a maximum of 2.4 wt. %). Interestingly, between the depths of 243.8 and 259.3 m, out of 25 samples 23 are below detection limit, yet between 259.3 and 406.58 m only one sample out of 71 was below detection limit, with values up to 4 wt.% (and one outlier at almost 6 wt.%). Sodium concentrations essentially change dramatically at around 259.3m and are often unexpectedly high below that depth. A lithological explanation has not yet been put forward, unless the thin mudstone acted as an impermeable barrier. However, there is no overall systematic smooth variation of Na_2O^* with either depth or $\delta^{18}O_{cal}$; for the depth range 259.3 to 319.52 m the respective r^2 values are 0.0327 (n=44) and 0.0033 (n=42), whereas by contrast the corresponding $\delta^{18}O_{cal}$ versus depth has a correlation statistically significant well above the 99% level. For the depth range 368.71 to 406.58 m, r^2 for Na_2O^* versus depth is 0.0062 (n=31) and Na_2O versus $\delta^{18}O_{cal}$ has r^2 of 0.0216 (n=30). On average, Na_2O^* values are higher for the deeper depth interval, and the range of values is also greater, consistent with a Na source at depth.

Intensive albitisation is seen in the solidified organic/siliceous mush in contact with the basin-wide ~70m thick basal gabbro (Unit B) at 414 m (Fig. 2D) and the timing of this intrusion is plausibly linked to the time of sedimentation of the C_{org}-rich rocks at the 156-132.59 m interval in 12AB, since there is evidence for seafloor seepage of migrated hydrocarbons (SFPS, Fig. 2) triggered by thermal maturation of organic matter at that time (Melezhik et al., 2013). In addition, halite and sylvinite micro-inclusions have been reported from the ZF

ACCEPTED MANUSCRIPT

organic-rich rocks by Kulikova (2013). Therefore Na was certainly available at this time. Recall also, that the gabbro must have been linked to a feeder system that would necessarily have interacted with the lithologies below ~400m, plausibly including the equivalent of the evaporites in the Tulomozero Formation reported by Krupenik et al. (2011). In conclusion, the Na distribution is consistent with the concept that it was established early and introduced from below. The lack of correlation between Na_2O^* and $\delta^{18}O_{cal}$ is therefore intriguing, arguably reflecting that the redistribution of sodium was linked to emplacement of the basin-wide gabbro, but that this was unrelated to the fluid-flow event responsible for oxygen isotope (re?)setting of calcite to the measured values. The latter may well have occurred sometime after the Svecofennian orogeny.

Conclusions

Sediments of the Palaeoproterozoic Zaonega Formation from the Onega Basin in Fennoscandia, sampled during the ICDP FAR-DEEP program, contain carbonates spanning 400m of stratigraphy. In particular, calcites display a wide range of petrographic styles and geochemistry. Notwithstanding such diversity, the oxygen isotopic composition ($\delta^{18}O_{cal}$) of the calcites throughout the full 400m has a strong linear anticorrelation with depth (z):

$$\mathbf{\delta^{18}O_{cal} = 17.3 - 13z \quad (r= 0.9495, n=178, >99.9\%).}$$

It is proposed that the calcite oxygen isotope ratios were reset by fluid-rock interaction. Under the assumption of a constant water isotopic composition ($\delta^{18}O_w$), the observed linear relationship is then explained by an increase in temperature with depth, according to the regional geothermal gradient. It is geologically implausible that this occurred during Svecofennian greenschist facies metamorphism. Rather, to account for $\delta^{18}O_{cal}$ decreasing by 5‰ over 400m requires a relatively near-surface situation for the rocks. Calculated values of $\delta^{18}O_w$ are <0‰ indicating a surface-derived fluid. For example, a surface temperature of 40°C and a geothermal gradient of 70°C km^{-1} then demands $\delta^{18}O_w$

ACCEPTED MANUSCRIPT

491 ~ -8.5‰. Alternatively, for a lower temperature of 15°C and a more modest
492 geothermal gradient of 52°C km^{-1} then $\delta^{18}O_w$ is calculated as ~ -13.6‰. It is
493 speculated that fluid infiltration was bedding-parallel rather than cross-
494 formational. The sodium distribution in the sediments suggests that Na has been
495 redistributed during fluid movement, but very plausibly in an earlier episode
496 than that responsible for the observed $\delta^{18}O_{cal}$ values.
497 The oxygen isotopic composition of carbonates in very ancient rocks is used, if at
498 all, usually for screening for processes which might have altered $\delta^{13}C$ and for
499 documenting metamorphic silicate-carbonate reactions (e.g. Valley, 1986). We
500 have shown here that, under exceptional circumstances, the carbonates can also
501 allow reconstruction of fluid-rock interactions, which allow constraints on such
502 important parameters as the extant geothermal gradient and the origin of the
503 fluid involved.
504
505 **Acknowledgements**
506
507
508 We acknowledge financial support from ICDP for the drilling programme. AEF,
509 ATB and ARP thank NERC for financial support through NE/G00398X/1. VAM,
510 AEC, and AL thank the Norwegian Research Council for financial support through
511 191530/V30. We are grateful for sample preparation and analyses to all the
512 personnel at NGU lab. At SUERC we enjoyed exceptional analytical support from
513 Julie Dougans. Two anonymous reviewers and the editor provided comments
514 that improved the final manuscript.
515
516
517 **References**
518
519 Cathles, L.M., Adams, J.J., 2005. Fluid flow and petroleum and mineral resources
520 in the upper (<20km) continental crust. Economic Geology 100th Anniversary
521 Volume pp. 77-110.
522

ACCEPTED MANUSCRIPT

523 Clauer, N., Honty, M., Fallick, A.E., Sucha, V., Aubert, A., 2014. Regional illitization
524 in bentonite beds from the East Slovak Basin based on isotopic characteristics
525 (K-Ar, $\delta^{18}O$ and δD) of illite-type nanoparticles. Clay Minerals, 49, 247-275.
526
527 Črne, A.E., Melezhik, V.A., Prave, A.R., Lepland, A., Romashkin, A.E., Rychanik, D.V.,
528 Hanski, E.J. and Luo, Zh.-Y., 2013a. Zaonega Formation: FAR-DEEP Holes 12A
529 and 12B, and neighbouring quarries. In: Melezhik, V.A., Prave, A.R., Fallick, A.E.,
530 Hanski, E.J., Lepland, A., Kump, L.R. and Strauss, H. (Eds.) Reading the Archive of
531 Earth's Oxygenation (Springer, Heidelberg) Vol. 2, pp.946-1007.
532
533 Črne, A.E., Melezhik, V.A., Prave, A.R., Lepland, A., Romashkin, A.E., Rychanik, D.V.,
534 Hanski, E.J. and Luo, Zh.-Y., 2013b. Zaonega Formation: FAR-DEEP Hole13A. In:
535 Melezhik, V.A., Prave, A.R., Fallick, A.E., Hanski, E.J., Lepland, A., Kump, L.R. and
536 Strauss, H. (Eds.) Reading the Archive of Earth's Oxygenation (Springer,
537 Heidelberg) Vol. 2, pp.1008-1046.
538
539 Črne, A.E., Melezhik, V.A., Lepland, A., Fallick, A.E., Prave, A.R. and Brasier, A.T.,
540 2014. Petrography and geochemistry of carbonate rocks of the
541 Palaeoproterozoic Zaonega Formation, Russia: documentation of ^{13}C-depleted
542 non-primary calcite. Precambrian Research 240, 79-93.
543
544 Egeberg, P.K. and Aagard, P., 1989. Origin and evolution of formation waters
545 from oil fields on the Norwegian shelf. Applied Geochemistry 4, 131-142.
546
547 Filippov, M.M., Golubev, A.I., Romashkin, A.E., Rychanchik, D.V., 1994. Mineral
548 constituent of shungite-bearing rocks: primary composition, sources and relation
549 to shungite matter. In: Filippov, M.M. (Ed.) The organic matter of Karelian
550 Shungite rocks (genesis, evolution, and the methods of study). Karelian Research
551 Centre, Petrozavodsk, pp. 78-93 (in Russian).
552
553 Friedman, I., O'Neil, J.R., 1977. Compilation of Stable Isotope Fractionation
554 Factors of Geochemical Interest. In: Fleischer, M. (Ed.) Data of Geochemistry,
555 Chapter KK, 6th edition. U.S. Geological Survey Professional Paper 440-KK.

ACCEPTED MANUSCRIPT

Haszeldine, R.S., Brint, J.F., Fallick, A.E., Hamilton, P.J., Brown, S., 1992. Open and restricted hydrologies in Brent Group diagenesis: North Sea. In: Morton, A.C., Haszeldine, R.S., Giles, M.R., Brown, S. (Eds.) Geology of the Brent Group, Geological Society of London Special Publication No. 61, pp. 401-409.

Jaffres, J.B.D., Shields, G.A., Wallmann, K., 2007. The oxygen isotopic composition of seawater: a critical review of a long-standing controversy and an improved geological water cycle model for the past 3.4 billion years. Earth-Science Reviews 83, 83-122.

Jenkin, G. R. T., Craw, D., Fallick, A. E., 1994. Stable isotopic and fluid inclusion evidence for meteoric fluid penetration into an active mountain belt; Alpine Schist, New Zealand. Journal of Metamorphic Geology 12, 429–444.

Koistnen, T., Stephens, M.B., Bogatchev, V., Nordgulen, Ø., Wennestrom, M., Kohrhonen, J. (comps), 2001. Geological Map of the Fennoscandian Shield, Scale 1 : 2 000 000, Espoo, Trondheim, Uppsala, Moscow.

Krupenik, V.A., Ahkmedov, A.M., Svshnikov, K.Yu., 2011. The section of the Onega structure based on the Onega parametric drillhole. In: Glushanin, L.V., Sharov, N.V., Shchiptsov, V.V. (Eds.) The Onega Palaeoproterozoic structure (Geology, tectonics, deep structure and minerageny). Karelian Research Centre, Petrozavodsk, pp.172-189 (in Russian).

Kulikova, V.V., 2013. Halite and sylvinite as chemical indicators of different-age basins (an example from the C_{org}-bearing sediments – shungites from SE Fennoscandia). In: Vakulenko, L.G., Jan, P.A. (Eds.), Sedimentary Basins, Sedimentary and Post-Sedimentary Processes in Geological History. Proceedings of the VII All-Russia Lithological Meeting, Novosibirsk, 28–31 October, 2013, p. 138–142.

ACCEPTED MANUSCRIPT

588 Melezhik, V.A., Fallick, A.E., Filippov, M., Deines, Y.E., Črne, A.E., Lepland, A.,
589 Brasier, A.T. and Strauss, H., 2013. Giant Palaeoproterozoic petrified oil field in
590 the Onega Basin. In: Melezhik, V.A., Kump, L.R., Fallick, A.E., Strauss, H., Hanski,
591 E.J., Prave, A.R. and Lepland, A. (Eds.) Reading the Archive of Earth's Oxygenation
592 (Springer, Heidelberg) Vol. 3, pp. 1202-1212.

593 Melezhik, V.A., Fallick, A.E., Brasier, A.T., Lepland, A., In press. Carbonate
594 deposition in the Palaeoproterozoic Onega basin from Fennoscandia: a spotlight on
595 the transition from the Lomagundi-Jatuli to Shunga events. Earth Science Reviews (*In*
596 *Press*).

597 Melezhik, V.A., Medvedev ,P.V. and Svetov, S.A., 2012. The Onega Basin. In:
598 Melezhik, V.A., Prave, A.R., Hanski, E.J., Fallick, A.E., Lepland, A., Kump, L.R. and
599 Strauss, H. (Eds.) Reading the Archive of Earth's Oxygenation (Springer,
600 Heidelberg) Vol. 1, pp. 387-490.

601 Puchtel, I.S., Arndt, N.T., Hofmann, A.W., Haase, K.M., Kröner, A., Kulikov, V.S.,
602 Kulikova, V.V., Garbe-Schönberg, C.-D., and Nemchin, A.A., 1998. Petrology on
603 mafic lavas within the Onega plateau, central Karelia: evidence for 2.0 Ga plume-
604 related continental crustal growth in the Baltic Shield. Contributions to
605 Mineralogy and Petrology 130, 134–153.
606
607 Puchtel, I.S., Zhuravlev, D.Z., Ashikhmina, N.A., Kulikov, V.S., and Kulikova, V.V.,
608 1992, Sm-Nd age of the Suisarian suite on the Baltic Shield, Transactions of
609 Russian Academy of Sciences 326: 706–711. (In Russian).
610
611 Qu, Y., Crne, A. E., Lepland, A., van Zuilen, M.A., 2012. Methanotrophy in a
612 Paleoproterozoic oil field ecosystem, Zaonega Formation, Karelia, Russia.
613 Geobiology 10, 467-478.
614
615 Sangster, D.F., Nowlan, G.S., McCracken, A.D., 1994. Thermal comparison of
616 Mississippi Valley-type lead-zinc deposits and their host-rocks using fluid
617 inclusion and conodont color alteration index data. Economic Geology, 89, 493-
618 514.

ACCEPTED MANUSCRIPT

Sheppard, S.M.F., 1986 Characterization and isotopic variations in natural waters. In: Valley J.W., Taylor H.P.,Jr. and O'Neil J.R. (Eds.) Reviews in Mineralogy Vol. 16, pp.165-183.

Sullivan, M.D., Haszeldine, R.S., Fallick, A.E., 1990. Linear coupling of carbon and strontium isotopes in Rotliegend Sandstone, North Sea; Evidence for cross-formational flow. Geology, 18, 1215-1218.

Urey, H.C., 1947. The thermodynamic properties of isotopic substances. J. Chem. Soc. (London), Part 1, 562-581.

Valley, J.W., 1986. Stable isotope geochemistry of metamorphic rocks. In: Valley, J.W., Taylor, H.P.,Jr., O'Neil, J.R. (Eds.) Stable Isotopes in High Temperature Geological Processes, Reviews in Mineralogy, Vol. 16, pp. 445-489.

Veizer, J., 1992. Depositional and diagenetic history of limestones: stable and radiogenic isotopes. In: Clauer, N., Chaudhuri, S. (Eds.) Isotopic Signatures and Sedimentary Records (Springer-Verlag, Berlin) pp. 13-48.

Volodichev, O.I., 1987. Metamorphism. In: Sokolov, V.A. (Ed.), Geology of Karelia. Nauka, Leningrad, pp. 152–175. (In Russian).

ACCEPTED MANUSCRIPT

ACCEPTED MANUSCRIPT

643 **Figure captions**

644

645 Figure 1. (A) Geographical location of the study area. (B) Simplified geological map
646 of the Onega Basin with the locations of FAR-DEEP Holes 12AB and 13A.
647 Geological map is based on Koistinen et al. (2001).

648

649 Figure 2. Stratigraphic variation of all carbonate Mg/Ca_{carb}, $\delta^{18}O_{carb}$ and $\delta^{13}C_{carb}$
650 values (symbols distinguished by calcite Mg/Ca_{carb} <0.1 and dolomite Mg/Ca_{carb} >0.1)
651 and Na_2O abundances in carbonate rocks based on Cores 12AB and 13A data.
652 Analytical data are from Črne et al. (2014) and FAR-DEEP database (http://far-
653 deep.icdp-online.org), and are documented in Tables 1 and 2.
654 FOT – fossil oil trap, SFPS – seafloor pyrobitumen seep, LMD – lowermost
655 dolostone. Depth in both cores in meters under the assumptions of core cross-
656 correlation explained in the text.

657

658 Figure 3. A depth versus $\delta^{18}O$ cross-plot for calcites (carbonates with Mg/Ca_{carb} <0.1
659 and so designated in the text as Mg/Ca_{cal}) studied in Core 12AB.

660

661 Fig. 4. Some illustrative and geologically possible values of temperature and
662 geothermal gradient satisfying equation [4].

663

664 Figure 5. Petrographic evidence of multiple calcitisation of dolostones in the ZF based
665 on Core 12AB. (A) Photomicrograph showing a dolostone injected by pyrobitumen
666 (black)-calcite (pink) vein. (B) Photomicrograph of a dolostone composed of
667 intergrown xenomorphic crystals of dolomite partially replaced by calcite (pink). (C)
668 Photomicrograph of a 'limestone' (Mg/Ca_{carb} = 0.03) composed of calcite (pink)-talc
669 (white) rock. (D) Scanned thin section showing pancake-like calcite (red) interpreted
670 as superimposed onto metamorphic fabrics of silty mudstone. (E) Photomicrograph of
671 porphyroblastic calcite (pink) apparently superimposed onto metamorphic fabrics of
672 arkosic sandstone. (F) Scanned Alizarin red-stained thin section showing bedding-
673 parallel calcitisation (pink) of selected beds in interbedded coarse-grained arkosic
674 sandstone (pink), organic-rich siltstone-sandstone (black) and fine-grained sericitic
675 quartzite (pale grey at the bottom). (G) Photomicrograpic profile through thin section

ACCEPTED MANUSCRIPT

detailing petrographic features of interbedded arkosic sandstone, siltstone-sandstone and quartzite shown in Fig. 5F. (H) Photomicrographic profile through thin section illustrating complete replacement of sandstones by porphyroblastic calcite. (I) Photomicrograph of interbedded fine- and coarse-grained arkosic sandstone. (J) Photomicrograph of thin section showing replacement of interbedded fine- and coarse-grained arkosic sandstone by porphyroblastic calcite.

A–E, I and G - photomicrographs of thin sections in non-polarised, transmitted light. J and H - photomicrographs of Alizarin red-stained thin sections in polarised, transmitted light. F – scanned, thin section.

ACCEPTED MANUSCRIPT

ACCEPTED MANUSCRIPT

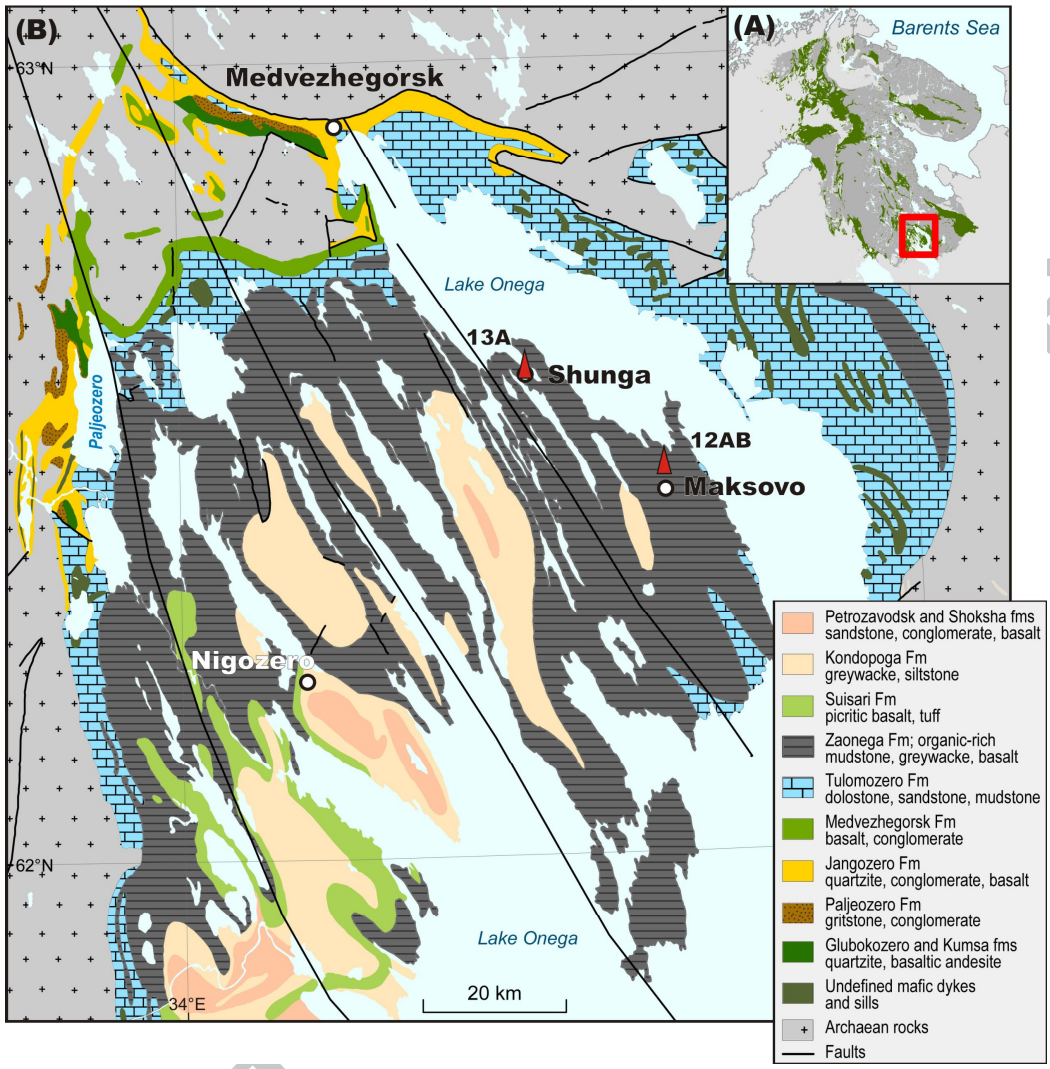

Fig. 1

ACCEPTED MANUSCRIPT

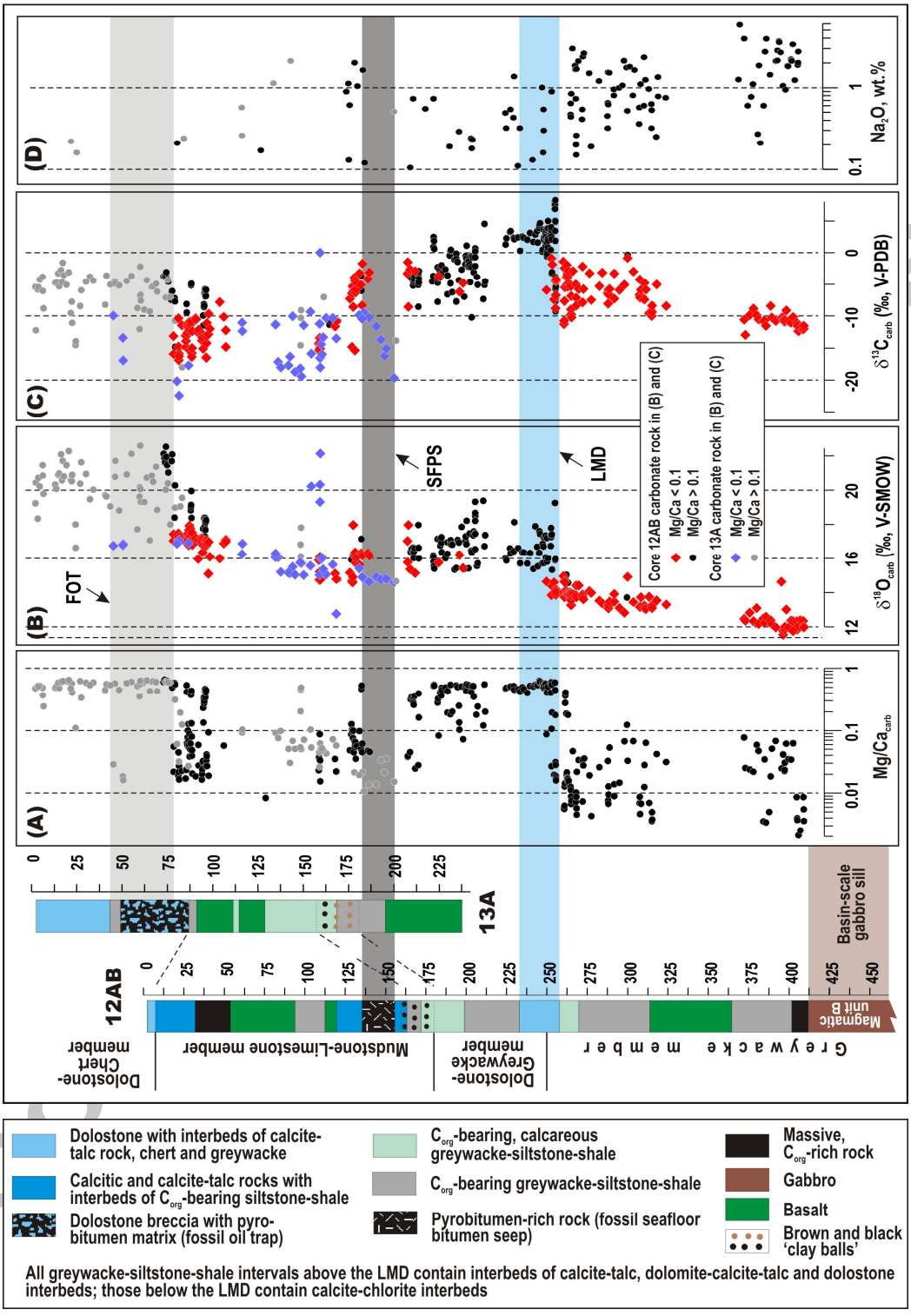

Fig. 2

ACCEPTED MANUSCRIPT

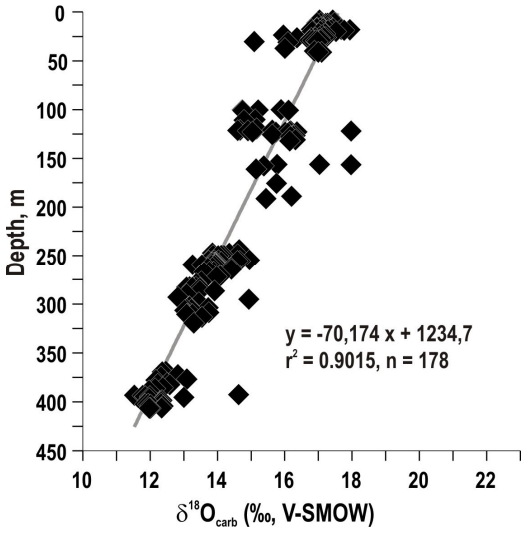

700

701

702

703 Fig. 3

704

705

ACCEPTED MANUSCRIPT

ACCEPTED MANUSCRIPT

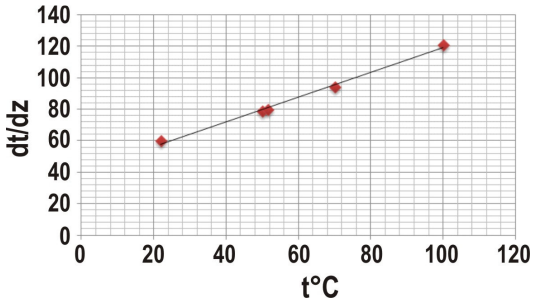

706

707

708 Fig. 4

709

710

ACCEPTED MANUSCRIPT

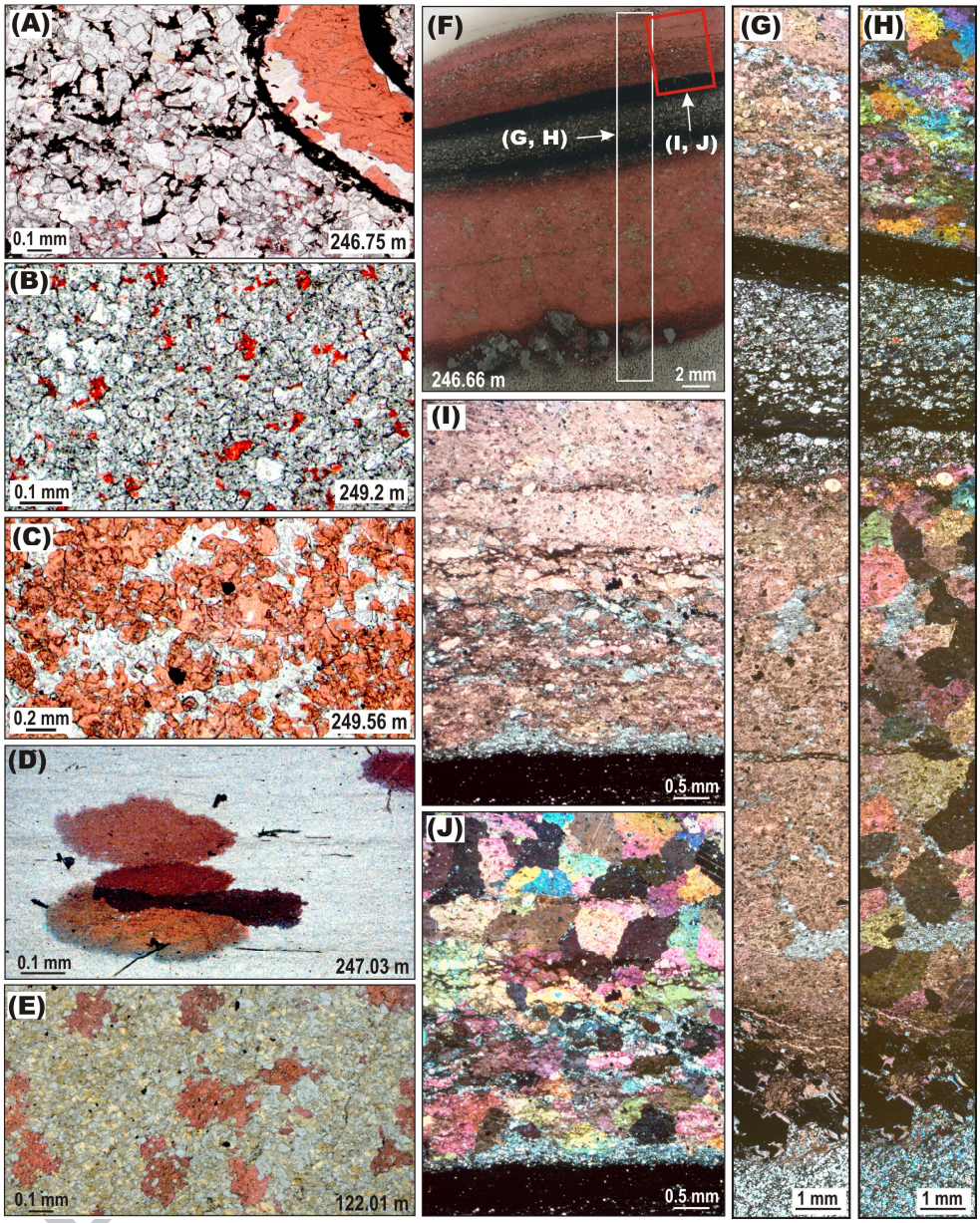

711
712
713
714 Fig. 5
715

ACCEPTED MANUSCRIPT

716 Table 1. Magnesium, calcium and sodium contents, and carbon (‰,V-PDB) and
717 oxygen (‰, V-SMOW) isotope values in calcites of the Zaonega Formation (Core
718 12AB).
719

#	Sample #	Depth, m	MgO_{wr}	CaO_{wr}	MgO/CaO	Na_2O	Mg_{carb}	Ca_{carb}	Mg/Ca	$\delta^{13}C$	$\delta^{18}O$
			wt.%			wt.%	μg g^{-1}				
1	3101838	8.11	4.61	37.5	0.12	<0.1	5610	256000	0.02	-13.1	17.0
2	3101840	8.22	4.50	40.0	0.11	<0.1	14900	269000	0.06	-15.9	17.4
3	3101946	11.14	6.90	32.2	0.21	<0.1	4140	218000	0.02	-14.8	17.5
4	3101948	11.23	8.73	23.7	0.37	<0.1	7290	163000	0.04	-10.3	17.1
5	3101950	11.37	11.7	23.2	0.50	<0.1	3410	157000	0.02	-16.9	17.0
6	3101952	11.54	14.8	25.2	0.59	<0.1	4660	171000	0.03	-15.9	17.2
7	3101954	11.6	8.16	31.5	0.26	<0.1	3500	212000	0.02	-16.3	17.3
8	3101960	13.32	5.96	20.6	0.29	0.21	3130	138000	0.02	-11.4	17.3
9	3101974	15.72	5.98	32.1	0.19	<0.1	3680	215000	0.02	-13.1	17.3
10	3101976	15.94	11.3	24.4	0.46	<0.1	3960	164000	0.02	-14.8	17.0
11	3101978	16.06	11.2	24.0	0.47	<0.1	3830	160000	0.02	-13.9	17.1
12	3101980	16.17	10.5	25.4	0.41	<0.1	3970	169000	0.02	-13.1	17.1
13	3101992	16.64	9.60	31.6	0.30	<0.1	13600	217000	0.06	-12.6	17.0
14	3101998	16.89	6.91	37.5	0.18	<0.1	14900	255000	0.06	-11.3	17.4
15	3102000	17.01	11.2	29.1	0.38	<0.1	15400	199000	0.08	-11.8	17.4
16	3102004	17.19	12.9	19.0	0.68	<0.1	13200	132000	0.10	-11.5	17.1
17	3102012	17.7	10.2	31.3	0.33	<0.1	14500	212000	0.07	-11.0	16.8
18	3102014	17.79	13.3	25.1	0.53	<0.1	9060	167000	0.05	-11.4	17.3
19	3102016	17.89	13.3	22.6	0.59	<0.1	9150	158000	0.06	-11.9	17.7
20	3102026	18.18	7.44	38.9	0.19	<0.1	22900	258000	0.09	-12.3	17.9
21	3102028	18.3	7.95	35.9	0.22	<0.1	9160	239000	0.04	-15.3	17.4
22	3102058	18.74	15.8	23.8	0.66	<0.1	8040	162000	0.05	-11.4	17.8
23	3102060	18.88	14.4	23.3	0.62	<0.1	9860	159000	0.06	-10.9	17.3
24	3102078	19.65	13.1	24.2	0.54	<0.1	13100	164000	0.08	-15.8	17.1
25	3102080	19.7	16.7	24.2	0.69	<0.1	6640	168000	0.04	-16.4	17.1
26	3102082	19.82	10.5	33.3	0.32	<0.1	10700	220000	0.05	-15.0	17.5
27	3102084	19.97	4.34	30.0	0.14	<0.1	4140	202000	0.02	-12.4	16.8
28	3102102	22.04	1.02	33.3	0.03	<0.1	4150	223000	0.02	-10.3	17.0
29	3113930	22.36	n.d.	n.d.	n.d.	n.d.	8700	120000	0.07	-10.5	17.2
30	3102106	23.79	9.31	23.5	0.40	<0.1	9190	156000	0.06	-12.6	16.0
31	3102108	23.95	9.07	23.5	0.39	<0.1	4420	160000	0.03	-12.1	17.1
32	3102132	26.02	6.66	38.4	0.17	<0.1	4330	263000	0.02	-13.8	17.2
33	3102134	26.14	9.00	34.7	0.26	<0.1	4880	240000	0.02	-13.3	17.2
34	3104572	26.23	10.3	34.0	0.30	<0.1	5700	236000	0.02	-12.8	17.0
35	3102142	26.42	18.1	21.4	0.85	<0.1	4590	146000	0.03	-13.2	16.4
36	3102144	26.55	14.7	28.8	0.51	<0.1	6220	198000	0.03	-13.4	16.9
37	3102146	26.68	15.8	25.5	0.62	<0.1	5820	179000	0.03	-15.1	16.8
38	3102186	28.74	15.5	27.8	0.56	<0.1	5110	190000	0.03	-16.4	16.7
39	3102188	28.83	23.1	15.0	1.54	<0.1	3440	103000	0.03	-16.5	17.0
40	3102190	28.95	19.8	20.0	0.99	<0.1	5840	141000	0.04	-14.2	17.1
41	3102192	29.1	17.4	20.4	0.85	<0.1	5380	139000	0.04	-13.2	16.8

ACCEPTED MANUSCRIPT

42	3102194	29.25	14.1	25.4	0.56	<0.1	4880	180000	0.03	-11.1	16.9
43	3102196	30.19	7.76	23.7	0.33	<0.1	14600	156000	0.09	-12.9	15.1

720 Table 1 (continued).
721

#	Sample #	Depth. m	MgO_{wr}	CaO_{wr}	MgO/CaO	Na_2O	Mg_{carb}	Ca_{carb}	Mg/Ca	$\delta^{13}C$	$\delta^{18}O$
			wt.%			wt.%	µg g^{-1}				
44	3102198	30.3	9.98	28.5	0.35	<0.1	3740	197000	0.02	-9.6	17.0
45	3113936	31.02	n.d.	n.d.	n.d.	n.d.	3060	34600	0.09	-12.0	16.1
46	3113938	37.22	n.d.	n.d.	n.d.	n.d.	3190	70600	0.05	-7.8	16.0
47	3102224	39.86	2.63	29.7	0.09	<0.1	11300	197000	0.06	-10.1	16.9
48	3113940	41.07	n.d.	n.d.	n.d.	n.d.	4800	176000	0.03	-12.2	17.1
49	3113942	41.2	n.d.	n.d.	n.d.	n.d.	4450	174000	0.03	-14.8	17.0
50	3113866	99.9	2.43	33.6	0.07	<0.1	5490	237000	0.02	-14.3	15.9
51	3102370	100.05	3.86	31.9	0.12	<0.1	8720	234000	0.04	-15.3	14.7
52	3102372	100.27	3.78	33.1	0.11	<0.1	10500	235000	0.04	-14.2	14.7
53	3102374	100.50	3.68	33.9	0.11	<0.1	19200	220000	0.09	-13.4	15.2
54	3113868	100.72	3.40	36.4	0.09	<0.1	8400	252000	0.03	-15.0	16.1
55	3102376	100.85	2.40	36.3	0.07	<0.1	3950	256000	0.02	-13.5	14.8
56	3102400	110.19	5.96	28.9	0.21	<0.1	7210	205000	0.04	-11.6	15.1
57	3102420	110.89	2.70	39.3	0.07	<0.1	6000	271000	0.02	-10.8	14.8
58	3102442	119.51	7.13	31.4	0.23	<0.1	10100	209000	0.05	-7.3	15.2
59	3102450	120.92	6.51	18.4	0.35	<0.1	12800	125000	0.10	-6.5	14.7
60	3102454	121.28	6.82	22.5	0.30	<0.1	15000	152000	0.10	-5.3	14.6
61	3102456	121.54	8.76	19.4	0.45	<0.1	9800	130000	0.08	-5.4	14.9
62	3102460	121.74	7.86	12.1	0.65	1.12	8080	81100	0.10	-8.5	18.0
63	3113876	122.01	6.28	26.5	0.24	0.13	8520	190000	0.04	-6.0	16.2
64	3113878	122.55	9.65	18.0	0.54	0.61	8530	127000	0.07	-3.9	16.1
65	3113880	122.86	8.64	26.4	0.33	<0.1	10900	187000	0.06	-4.4	16.4
66	3113882	123.07	6.13	24.3	0.25	<0.1	11100	171000	0.06	-6.3	15.7
67	3113884	123.3	4.09	34.8	0.12	<0.1	8660	245000	0.04	-5.8	16.0
68	3113886	123.96	7.08	25.3	0.28	<0.1	9870	175000	0.06	-4.9	16.1
69	3113888	125.65	6.20	16.1	0.39	2.00	10900	111000	0.10	-3.2	15.6
70	3113892	126.61	8.46	31.1	0.27	<0.1	10700	214000	0.05	-5.1	16.3
71	3113894	127.24	10.20	27.7	0.37	<0.1	8430	187000	0.05	-8.3	16.3
72	3113896	127.46	7.29	17.2	0.42	1.04	7400	120000	0.06	-1.7	16.2
73	3113898	130.96	3.28	22.5	0.15	1.63	7290	154000	0.05	-4.2	16.3
74	3113900	132.07	3.80	29.0	0.13	0.12	9160	201000	0.05	-3.1	16.2
75	3102562	156.12	4.43	24.6	0.18	<0.1	6160	162000	0.04	-3.3	17.0
76	3102564	156.24	3.28	28.1	0.12	<0.1	7380	188000	0.04	-1.5	15.8
77	3102566	156.5	9.81	8.0	1.23	0.25	3760	52300	0.07	-8.5	18.0
78	3102568	157.6	4.53	39.0	0.12	<0.1	11900	264000	0.05	-2.7	15.4
79	3102592	160.86	4.42	30.5	0.14	0.10	5170	209000	0.02	-2.9	15.1
80	3113840	175.66	4.99	10.6	0.47	0.73	6160	74100	0.08	-3.7	15.8
81	3102688	188.87	4.74	27.8	0.17	<0.1	19600	190000	0.10	-6.2	16.2
82	3102696	191.12	4.27	23.2	0.18	<0.1	11600	160000	0.07	-4.8	15.4
83	3113784	243.82	13.70	11.3	1.21	<0.1	6910	79300	0.09	-5.9	14.6
84	3102886	247.03	14.00	24.3	0.58	<0.1	4680	174000	0.03	-0.9	13.9

ACCEPTED MANUSCRIPT

ACCEPTED MANUSCRIPT

85	3102900	247.44	8.01	7.0	1.14	2.37	3170	50900	0.06	-1.9	14.4
86	3102904	248.7	1.19	12.1	0.10	<0.1	1740	88500	0.02	-7.4	14.6
87	3102912	249.56	19.10	21.2	0.90	<0.1	4550	145000	0.03	-8.8	14.1

Table 1 (continued).

#	Sample #	Depth. m	MgO_{wr}	CaO_{wr}	MgO/CaO	Na_2O	Mg_{carb}	Ca_{carb}	Mg/Ca	$\delta^{13}C$	$\delta^{18}O$
			wt.%			wt.%	µg g^{-1}				
88	3102914	249.65	18.80	22.0	0.85	<0.1	4190	148000	0.03	-6.7	13.9
89	3102916	249.73	14.70	27.8	0.53	<0.1	3670	196000	0.02	-4.5	14.2
90	3102918	249.8	14.10	27.3	0.52	<0.1	3300	195000	0.02	-4.3	14.1
91	3102920	249.85	7.38	29.5	0.25	<0.1	3300	207000	0.02	-4.2	14.0
92	3102942	254.46	10.80	9.4	1.15	2.41	2490	66700	0.04	-1.4	15.0
93	3102946	254.83	1.24	50.3	0.02	<0.1	1900	325000	0.006	-11.3	13.9
94	3102948	254.95	1.99	50.2	0.04	<0.1	1960	352000	0.006	-10.7	14.0
95	3102952	255.2	3.08	48.6	0.06	<0.1	2190	348000	0.006	-7.6	13.7
96	3102954	255.34	12.00	34.0	0.35	<0.1	3050	239000	0.013	-2.4	14.7
97	3102956	255.48	14.50	29.1	0.50	<0.1	2970	207000	0.014	-5.5	14.6
98	3102966	256.52	12.00	33.6	0.36	<0.1	4670	238000	0.02	-3.8	14.1
99	3102968	256.74	17.50	21.8	0.80	<0.1	3370	158000	0.02	-1.9	14.0
100	3102970	256.96	17.70	21.8	0.81	<0.1	2690	154000	0.02	-5.0	13.9
101	3102972	257.08	14.10	30.2	0.47	<0.1	3410	209000	0.02	-3.9	13.8
102	3102974	257.2	13.00	31.8	0.41	<0.1	3850	222000	0.02	-3.6	13.9
103	3102976	257.29	13.70	33.7	0.41	<0.1	3590	214000	0.02	-5.4	14.0
104	3102980	257.71	11.50	33.3	0.35	<0.1	3380	232000	0.015	-4.9	13.8
105	3102982	257.85	9.49	32.0	0.30	<0.1	3480	221000	0.02	-2.9	14.0
106	3102990	258.97	3.90	44.8	0.09	<0.1	3870	311000	0.012	-5.1	14.0
107	3102992	259.11	4.01	46.1	0.09	<0.1	3890	310000	0.013	-5.3	14.0
108	3102994	259.3	4.19	37.6	0.11	0.47	2960	265000	0.011	-9.0	13.9
109	3102996	259.39	0.86	48.1	0.02	0.64	2910	329000	0.009	-9.7	13.3
110	3102998	259.47	0.72	48.0	0.02	0.44	2310	343000	0.007	-6.8	13.5
111	3103000	259.7	0.76	44.2	0.02	0.84	2360	310000	0.008	-10.2	13.8
112	3103006	260.48	1.77	12.0	0.15	2.97	4070	86900	0.05	-2.9	13.9
113	3103012	262.4	0.59	35.7	0.02	1.66	1880	259000	0.007	-5.0	13.9
114	3103014	262.57	0.82	48.6	0.02	0.73	3500	342000	0.010	-7.1	14.4
115	3103016	262.69	0.63	52.4	0.01	0.20	3280	375000	0.009	-8.3	13.7
116	3113794_1	264.2	3.52	27.0	0.13	2.09	6330	187000	0.03	-5.8	14.4
117	3103034	266.54	4.40	30.2	0.15	0.41	7600	222000	0.03	-2.2	13.9
118	3103036	266.67	0.60	48.1	0.01	0.54	2570	349000	0.007	-7.8	13.8
119	3103046	267.10	2.92	27.4	0.11	2.37	5040	182000	0.03	-5.8	13.6
120	3113806	271.06	1.82	37.6	0.05	1.49	5020	261000	0.02	-3.2	14.1
121	3113808	272.24	0.39	48.6	0.01	0.19	1460	339000	0.004	-7.5	14.0
122	3103096	277.28	2.85	28.7	0.10	1.20	5470	211000	0.03	-5.3	13.5
123	3103100	279.03	1.47	4.6	0.32	0.42	2800	34300	0.08	-3.1	13.4
124	3103118	282.65	2.89	34.6	0.08	0.45	8070	247000	0.03	-6.4	13.2
125	3103120	282.78	1.11	48.9	0.02	0.32	2640	345000	0.008	-8.0	13.3
126	3103122	282.9	1.30	47.1	0.03	0.65	2270	335000	0.007	-6.5	13.4
127	3103124	283.02	2.99	35.1	0.09	1.53	3220	252000	0.013	-5.9	13.1

ACCEPTED MANUSCRIPT

128	3103126	283.15	1.81	44.0	0.04	0.62	2930	309000	0.009	-6.7	13.3
129	3113716	283.72	7.56	18.0	0.42	1.51	6520	122000	0.05	-5.8	13.5
130	3113720_3	286.65	2.34	40.8	0.06	0.95	2550	284000	0.009	-3.3	13.5
131	3113720_1	286.65	2.70	40.5	0.07	0.80	4040	291000	0.014	-7.3	13.9

Table 1 (continued).

#	Sample #	Depth. m	MgO_{wr}	CaO_{wr}	MgO/CaO	Na_2O	Mg_{carb}	Ca_{carb}	Mg/Ca	$\delta^{13}C$	$\delta^{18}O$
			wt.%			wt.%	$\mu g\ g^{-1}$				
132	3103146	289.96	4.65	32.5	0.14	0.99	3360	229000	0.015	-5.9	13.1
133	3103162	293.12	6.33	15.9	0.40	2.11	7540	112000	0.07	-5.1	12.8
134	3113724	295.2	7.47	20.5	0.36	0.52	4600	140000	0.03	-0.8	14.9
135	3113728	298.71	10.20	12.5	0.82	0.80	5570	82200	0.07	-3.0	13.5
136	3103188	302.7	3.30	41.8	0.08	0.36	2040	294000	0.007	-6.7	13.2
137	3103190	302.83	4.17	38.0	0.11	0.57	2340	268000	0.009	-4.2	13.2
138	3103254	303	1.22	50.5	0.02	<0.1	1660	358000	0.005	-7.1	13.2
139	3113730	303.63	1.95	42.3	0.05	1.10	1980	292000	0.007	-5.9	13.7
140	3103200	305.7	5.14	34.4	0.15	0.60	3120	249000	0.013	-7.4	13.2
141	3103202	305.79	5.43	17.7	0.31	2.33	3570	127000	0.03	-4.8	13.1
142	3113732	306.68	9.40	10.3	0.91	1.24	4310	67800	0.06	-5.9	13.0
143	3113734	308.78	2.17	41.2	0.05	0.96	1970	282000	0.007	-9.6	13.7
144	3103208	310.43	2.57	43.2	0.06	0.63	1010	283000	0.004	-10.0	13.1
145	3103210	310.55	3.43	41.4	0.08	0.32	1460	295000	0.005	-9.4	13.3
146	3103212	310.67	1.91	46.6	0.04	0.53	1240	328000	0.004	-8.4	13.1
147	3113736	313.49	10.00	12.2	0.82	0.25	3450	81800	0.04	-5.0	13.5
148	3113742	319.52	7.34	16.1	0.46	0.75	3420	109000	0.03	-8.4	13.3
149	3113688	368.71	10.80	11.2	0.96	1.25	4490	58000	0.08	-10.6	12.5
150	3113690	369.51	4.31	10.1	0.43	5.79	1200	47600	0.03	-12.9	12.4
151	3113694	372.33	4.72	20.1	0.23	3.92	2760	116000	0.02	-9.8	12.8
152	3103294	374.58	6.85	21.9	0.31	0.60	3200	146000	0.02	-8.8	12.3
153	3113696	376.74	9.65	13.6	0.71	0.77	5240	89000	0.06	-9.9	13.1
154	3103308	377.9	7.41	13.6	0.54	1.10	4370	92500	0.05	-10.5	12.2
155	3113698	380.96	2.00	42.6	0.05	0.27	1050	297000	0.004	-10.8	12.5
156	3113710	381.7	6.16	20.3	0.30	1.85	4840	140000	0.035	-10.7	12.2
157	3113712	382.58	1.78	42.3	0.04	0.21	987	291000	0.003	-11.5	12.6
158	3103326	385.55	2.58	32.9	0.08	2.72	4370	236000	0.02	-8.4	12.4
159	3113642	386.37	5.11	11.6	0.44	3.91	3600	70100	0.05	-10.2	12.1
160	3103332	388.7	9.06	16.3	0.56	1.43	7370	108000	0.07	-10.8	12.0
161	3113646	392.44	5.87	23.7	0.25	2.10	3940	159000	0.02	-10.3	14.6
162	3103340	393.34	4.18	19.6	0.21	2.13	5270	126000	0.04	-10.2	11.5
163	3103342	393.45	4.55	16.6	0.27	2.82	4730	115000	0.04	-10.6	11.8
164	3103352	394.3	4.83	21.0	0.23	3.66	3210	143000	0.02	-10.5	11.9
165	3103354	394.42	4.85	21.2	0.23	3.64	3420	146000	0.02	-10.9	11.9
166	3103356	394.54	5.79	18.6	0.31	3.54	3710	121000	0.03	-10.7	12.0
167	3113650	395.36	4.88	13.5	0.36	2.67	5040	81800	0.06	-9.1	13.0
168	3103364	396.88	4.90	27.6	0.18	1.05	6660	191000	0.03	-10.8	12.0
169	3113652	398.49	5.17	25.0	0.21	0.94	5750	168000	0.03	-11.0	12.4
170	3113654	399.75	5.33	18.9	0.28	1.83	7680	123000	0.06	-10.2	12.3

ACCEPTED MANUSCRIPT

171	3113658	401.99	1.38	36.5	0.04	2.20	2140	248000	0.009	-11.1	12.3
172	3103378	402.33	1.11	40.1	0.03	2.13	1100	278000	0.004	-11.5	11.9
173	3103380	402.42	1.54	38.3	0.04	2.10	956	258000	0.004	-11.5	11.9
174	3103384	403.15	1.47	30.9	0.05	3.34	410	197000	0.002	-12.4	12.0
175	3113664	404.34	0.99	43.4	0.02	1.23	731	292000	0.003	-11.9	12.4

Table 1 (continued).

#	Sample #	Depth. m	MgO_{wr}	CaO_{wr}	MgO/CaO	Na_2O	Mg_{carb}	Ca_{carb}	Mg/Ca	$\delta^{13}C$	$\delta^{18}O$
			wt.%			wt.%	µg g^{-1}				
176	3103400	406.25	3.24	35.4	0.09	1.88	1800	208000	0.009	-12.1	12.3
177	3103402	406.45	2.78	34.0	0.08	2.00	1240	225000	0.006	-12.0	12.0
178	3103404	406.58	1.86	34.2	0.05	2.73	825	231000	0.004	-11.5	12.0

n.d. – not determined.
MgO, MgO and Na_2O are determined by XRF in whole-rock samples, whereas Mg and Ca by ICP-AES in acid-soluble components.

ACCEPTED MANUSCRIPT

ACCEPTED MANUSCRIPT

Table 2. Magnesium, calcium and sodium contents, and carbon (‰,V-PDB) and oxygen (‰, V-SMOW) isotope values in calcites of the Zaonega Formation (Core 13AB).

#	Sample #	Depth, m	MgO_{wr}	CaO_{wr}	MgO/CaO	Na_2O	Mg_{carb}	Ca_{carb}	Mg/Ca	$\delta^{13}C$	$\delta^{18}O$
			wt.%			wt.%	μg g^{-1}				
1	3113490	43.81	11.2	14.5	0.77	<0.1	3090	107000	0.03	-9.9	16.7
2	3113494	48.80	9.43	27.9	0.34	<0.1	3780	204000	0.02	-13.4	16.8
3	3113496	49.06	5.88	33.8	0.17	<0.1	3900	242000	0.02	-16.9	16.9
4	3113580	77.85	9.98	27.4	0.36	<0.1	12100	199000	0.06	-20.2	16.9
5	3113582	78.85	7.74	30.3	0.26	<0.1	7110	223000	0.03	-22.4	17.1
6	3113584	83.97	5.61	19.3	0.29	0.24	3870	143000	0.03	-17.7	16.9
7	3104968	112.69	3.45	10.1	0.34	0.57	7210	77700	0.09	-11.0	16.3
8	3113468	112.83	4.59	11.1	0.41	0.26	8660	83800	0.10	-12.3	16.9
9	3113472	130.49	2.51	7.74	0.32	0.84	5550	57700	0.10	-11.4	16.3
10	3113474	130.58	3.84	10.9	0.35	1.13	7260	79500	0.09	-11.3	16.1
11	3105000	132.02	12.1	29.3	0.41	<0.1	16100	212000	0.08	-17.1	16.1
12	3105006	133.34	9.62	18.4	0.52	<0.1	13300	135000	0.10	-18.1	15.2
13	3105022	137.53	8.04	22.5	0.36	<0.1	8760	172000	0.05	-17.7	15.2
14	3105024	138.33	5.50	30.5	0.18	<0.1	6860	226000	0.03	-16.3	15.1
15	3113488	139.77	4.46	11.8	0.38	2.10	5910	86500	0.07	-10.0	15.5
16	3105032	141.02	14.3	24.2	0.59	<0.1	8970	176000	0.05	-18.7	15.0
17	3113406	143.89	11.3	28.5	0.40	<0.1	11200	208000	0.05	-18.1	15.8
18	3113412	144.39	14.7	23.8	0.62	<0.1	8690	172000	0.05	-19.4	15.7
19	3105044	145.78	7.22	18.7	0.39	<0.1	9940	140000	0.07	-11.4	15.0
20	3113414	149.32	12.2	12.1	1.01	<0.1	9180	88800	0.10	-9.3	15.6
21	3105060	149.73	10.1	28.0	0.36	<0.1	10900	204000	0.05	-15.9	20.2
22	3113416	154.15	4.28	37.9	0.11	<0.1	7300	279000	0.03	-11.2	15.0
23	3113418	154.31	12.7	26.1	0.49	<0.1	8610	192000	0.04	-16.5	19.3
24	3105078	154.47	12.7	21.0	0.60	<0.1	9400	151000	0.06	0.0	20.3
25	3113420	154.59	13.0	23.4	0.56	<0.1	8290	168000	0.05	-18.0	22.1
26	3113422	155.04	8.22	32.9	0.25	<0.1	11500	238000	0.05	-14.4	15.9
27	3113424	155.43	8.82	33.2	0.27	<0.1	12400	238000	0.05	-16.0	16.0
28	3105086	156.10	4.57	30.4	0.15	<0.1	11000	226000	0.05	-13.3	15.4
29	3113426	157.71	4.62	26.1	0.18	<0.1	8200	191000	0.04	-10.3	15.1
30	3105100	161.22	7.11	22.7	0.31	<0.1	12100	167000	0.07	-10.3	15.6
31	3105104	163.07	9.73	26.2	0.37	<0.1	10700	186000	0.06	-13.5	12.8
32	3105146	175.41	2.86	42.9	0.07	<0.1	5950	306000	0.02	-9.8	15.4
33	3105152	177.02	2.30	37.6	0.06	<0.1	5930	275000	0.02	-10.4	14.9
34	3105154	177.95	2.02	46.3	0.04	<0.1	3790	353000	0.01	-9.5	14.8
35	3105160	180.61	2.95	44.1	0.07	<0.1	4640	342000	0.01	-10.2	14.6
36	3105176	184.55	2.14	45.8	0.05	<0.1	4890	355000	0.01	-11.6	14.9
37	3113452	187.03	4.25	33.5	0.13	<0.1	8960	266000	0.03	-13.7	14.8
38	3113456	188.87	2.93	38.4	0.08	<0.1	6640	309000	0.02	-16.2	14.8
39	3113458	189.89	3.95	31.1	0.13	<0.1	9290	263000	0.04	-15.1	14.8
40	3105222	194.12	1.38	46.4	0.03	<0.1	5510	362000	0.02	-19.7	14.6

MgO, MgO and Na_2O are determined by XRF in whole-rock samples, whereas Mg and Ca by ICP-AES in acid-soluble components.

ACCEPTED MANUSCRIPT

RESEARCH HIGHLIGHTS

- All calcite $\delta^{18}O$ values lie close to a single linear depth trend.
- this is interpreted as oxygen isotope resetting by fluid-rock interaction
- depth trend of $\delta^{18}O$ was controlled by a high ancient geothermal gradient.

ACCEPTED MANUSCRIPT